

SELECTIVE CORROSION OF Al₂Cu INTERMETALLIC PHASE IN ORTHOPHOSPHORIC ACID AQUEOUS SOLUTIONS

Al₂Cu phase has been obtained by melting pure metals in the electric arc furnace. It has been found that the intermetallic phase undergoes selective corrosion in the H₃PO₄ aqueous solutions. Aluminium is dissolved, the surface becomes porous and enriched with copper. The corrosion rate equals to $371 \pm 17 \text{ g} \cdot \text{m}^{-2} \cdot \text{day}^{-1}$ (aerated solution) and $284 \pm 9 \text{ g} \cdot \text{m}^{-2} \cdot \text{day}^{-1}$ (deaerated solution). The surface of Al₂Cu phase after selective corrosion was characterised by using electrochemical impedance spectroscopy. It was found that the surface area of the specimens increases with temperature due to higher corrosion rate and is between 2137 and 3896 cm².

Keywords: intermetallic phase; selective corrosion; orthophosphoric acid; electrochemical impedance spectroscopy

1. Introduction

Microstructure of wrought aluminium alloys is complex and composed of several intermetallic phases. One of the most important is Al₂Cu. According to the Al-Cu phase diagram, it is formed in the peritectic reaction, at 873 K [1]. Al₂Cu phase is hard and ensures good strength of precipitation hardened Al-Cu-Mg-Mn alloys, as well as Al-Cu alloy-based metal matrix composites [2].

Al₂Cu phase is more noble when compared to Al-based solid solution, regardless of the pH of the environment [3-5]. The particles of this phase constitute the local cathodes in the galvanic cells, where the reduction of O₂ or H₃O⁺ occurs. The overpotential of both cathodic processes on Al₂Cu is lower when compared to Al. Therefore, fine precipitates of Al₂Cu phase, within the matrix of Cu-rich aluminium alloys, deteriorate their corrosion resistance significantly [3]. The corrosion behaviour of Al₂Cu phase itself was mainly evaluated in the chloride media. It was shown that the intermetallic phase remains passive in 0.1 M NaCl aqueous solution in the wide range of pH (2.5-12) [4]. Similar results were obtained in the borate buffer. However, when the exposition time was sufficiently long, its surface became enriched with copper [3]. The selective corrosion of Al₂Cu is much more severe in 10 wt. % NaOH [6] and 2 M H₂SO₄ [7].

In general, dealloying of alloys significantly deteriorates their various properties, for instance, yield stress and ductility of brass and cast iron [8], electrocatalytic activity towards hydrogen evolution of ferrous alloys [9]. On the one hand, dealloying of the intermetallic phases negatively influences the corrosion behaviour and anodising process of Cu-rich aluminium alloys

[7]. On the other hand, this process can be utilised for synthesis of nanoporous materials [6].

In this work, the corrosion of Al₂Cu intermetallic phase in orthophosphoric acid aqueous solution has been studied for the first time. It is important from practical point of view, since H₃PO₄ is used *e.g.* for etching of aluminium alloys as the pre-treatment step for anodisation. Detailed knowledge of the corrosion behaviour of the intermetallic phases in acidic solutions is useful for better understanding of the behaviour of aluminium alloys during etching and application of the appropriate corrosion inhibitors.

2. Experimental

The Al₂Cu electrodes with three different content of copper were obtained by the electric arc melting process of Al and Cu (99.999 wt. % purity). It was carried out in water-cooled copper crucibles, by using a tungsten electrode, in the atmosphere of Ar ($p = 60 \text{ kPa}$). Then they were annealed ($T = 823 \text{ K}$, $t = 24 \text{ h}$), cut by using the electrical discharge machine to 10 mm diameter specimens and mounted in the epoxy resin.

The characterisation of the electrodes included determination of their chemical (ARL ADVANT' XP Sequential X-ray Fluorescence Spectrometer, Thermo Scientific) and phase (ARL X'Tra X-ray diffractometer, Cu K_α radiation source) composition as well as microstructure (Leica DM 3000 light microscope, HITACHI S-3400N Scanning Electron Microscope). Prior microscopic examination, specimens were etched in diluted hydrofluoric acid (0.5 cm³ HF (48 wt.%) and 99.5 cm³ H₂O). The chemical composition of the solutions after the corrosion process

* RZESZOW UNIVERSITY OF TECHNOLOGY, DEPARTMENT OF MATERIALS SCIENCE, 12 POWSTAŃCÓW WARSZAWY AV, 35-959 RZESZÓW, POLAND

Corresponding author: pkwolek@prz.edu.pl

was determined by using the inductively-coupled plasma optical emission spectroscopy ICP-OES (Ultima 2 Horiba Jobin Yvon).

Prior the electrochemical examination, the Al_2Cu electrodes (0.79 cm^2) were abraded by a sandpaper (grit 320 and 500), washed with water, isopropyl alcohol and dried with compressed air. The electrochemical research were conducted in the standard, three electrode setup (graphite counter electrode, Ag/AgCl 3 M KCl reference electrode), by using Bio-Logic SP-300 potentiostat, in 100 cm^3 of $0.5 \text{ M H}_3\text{PO}_4$ aqueous solution, at 295, 300 and 307 K.

The corrosion potential of Al_2Cu phase was determined after 20 h of exposition in the solution. The impedance spectra were then recorded in the frequency range between 200 kHz and 10 mHz and approximated with the equivalent circuit (*vide*

infra) by using the Zview software (Scribner Associates). The experiments were repeated 3 times. Data points in the graphs represent the average of 3 values. Their uncertainties u were then calculated (Eq. (1)):

$$u = t \frac{SD}{\sqrt{3}} \quad (1)$$

where SD is the standard deviation of the averaged value, $t = 2.92$ (90% confidence level). The potentiodynamic polarisation curves were determined at the scanning rate of $5 \text{ mV} \cdot \text{min}^{-1}$ for aerated and deaerated solution in the vicinity ($\pm 25 \text{ mV}$) of the corrosion potential. The anodic polarisation curves, in turn, were recorded at the scanning rate of $0.5 \text{ mV} \cdot \text{s}^{-1}$.

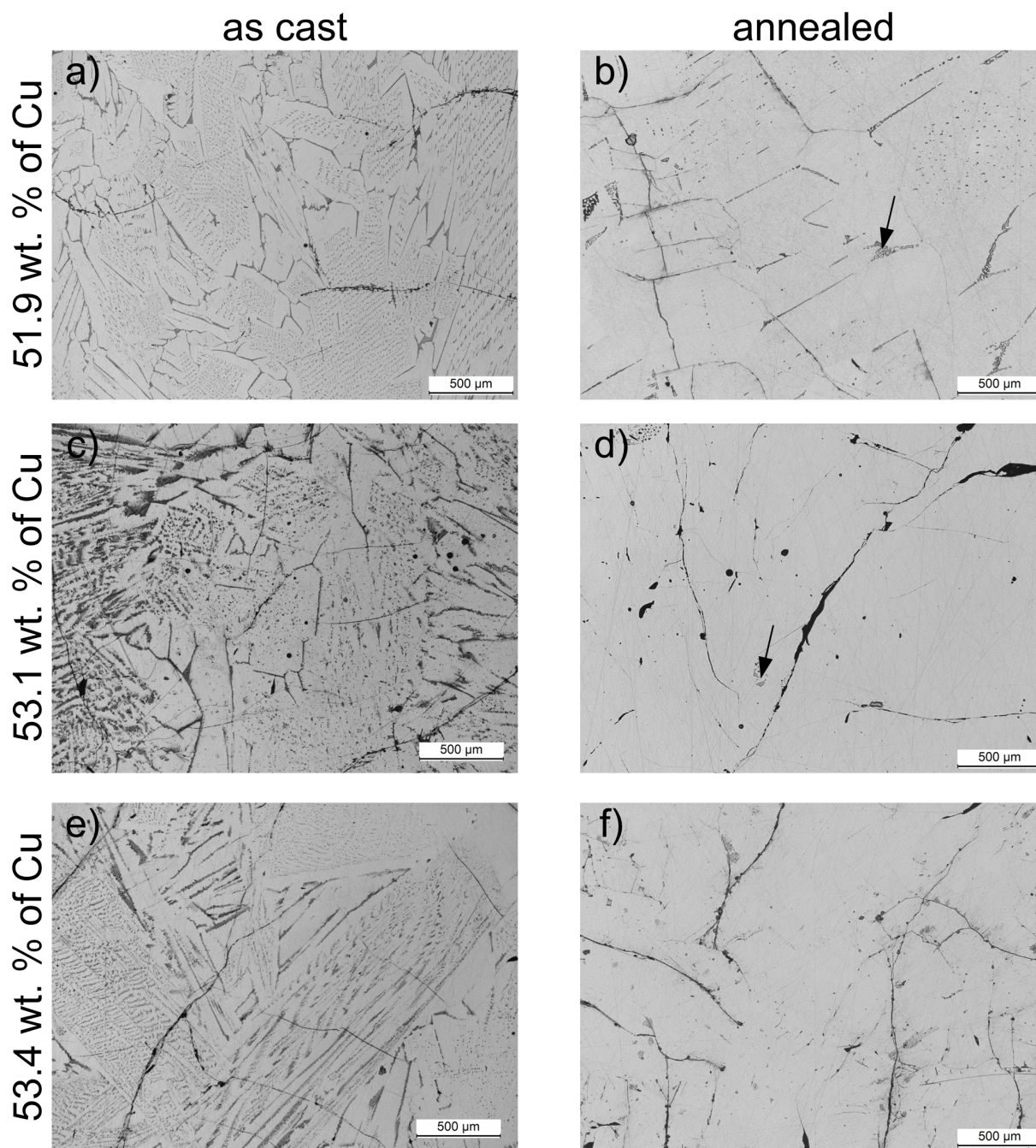


Fig. 1. The microstructure of the specimens as a function of their chemical composition, after casting a), c), e) and subsequent annealing at 823 K for 24 hours b), d), f), arrows indicate the remaining of the eutectic mixture in the microstructure

3. Results and discussion

3.1. The microstructure and phase composition of the Al₂Cu phase

The content of copper in the three Al-Cu alloys obtained in the arc melting process was the following: 49.5, 51.2 and 51.9 wt. %. It should be noted here that the maximal range of stability of Al₂Cu phase is between 51.9 and 53.4 wt. % of Cu. Microscopic characterisation of the as-cast alloys (without annealing) revealed that their microstructure is composed of the eutectic mixture of Al₂Cu and Al(Cu) solid solution crystals, together with the hypereutectic crystals of the Al₂Cu phase (Fig. 1a, c, e). Since the cooling rate was very high and the crystallisation occurred under non-equilibrium conditions, the specimens were annealed for 24 hours, in order to achieve the equilibrium microstructure. The heat treatment applied reduced the relative volume of the eutectic mixture in the microstructure (Fig. 1b, d, f). Virtually single-phase alloy was obtained for the highest concentration of copper (Fig. 1f). Therefore, this alloy was applied in the subsequent corrosion experiments.

The phase composition of the obtained materials was also confirmed by using the X-ray diffraction method (Fig. 2). All the diffraction lines obtained were ascribed to the Al₂Cu phase (ICDD 04-001-0923 card). The diffraction lines characteristic for aluminium (2θ equal to 38.47°; 44.74°; 65.13° and 77.22°) were not found. It was also observed that the intensities of diffraction lines differ between the specimens. It is due to the big grain size of the prepared alloys.

3.2. The mechanism of corrosion of Al₂Cu phase

The corrosion rate of Al₂Cu phase in 0.5 M H₃PO₄ aqueous solution was calculated on the basis of the concentration of aluminium and copper in the solution, after 20.4 hours of immersion (Table 1). The following results were obtained:

$284 \pm 9 \text{ g} \cdot \text{m}^{-2} \cdot \text{day}^{-1}$ for deaerated and $371 \pm 17 \text{ g} \cdot \text{m}^{-2} \cdot \text{day}^{-1}$ for aerated solution. When the solution is deaerated, almost only Al atoms are leached. Oxygen dissolved in the solution act as an additional depolariser and increases the corrosion rate. In addition, more copper is dissolved when compared to the former case. It can be concluded that the corrosion rate of Al₂Cu phase is very high when compared to aluminium 1050 or 2024 alloy immersed in the same solution (*c.a.* $15 \text{ g} \cdot \text{m}^{-2} \cdot \text{day}^{-1}$ [10,11]).

TABLE 1

Concentration of aluminium and copper in the solutions, determined by using ICP-OES, immersion time 20.4 h, $T = 300 \text{ K}$

Element	Concentration in the solution	
	purged with Ar	in equilibrium with air
Aluminium	$193.00 \pm 5.84 \text{ mg} \cdot \text{dm}^{-3}$	$250.70 \pm 11.48 \text{ mg} \cdot \text{dm}^{-3}$
Copper	$57.3 \pm 8.2 \text{ } \mu\text{g} \cdot \text{dm}^{-3}$	$1110.0 \pm 16.8 \text{ } \mu\text{g} \cdot \text{dm}^{-3}$

The examination of the surface of Al₂Cu specimen with SEM confirmed that Al₂Cu phase underwent selective corrosion (Fig. 3a and b, Table 2). The surface became porous and significantly enriched with copper due to dissolution of aluminium. Parts of this porous structure can be mechanically detached from the surface and dissolve in the solution containing oxygen. It is probably responsible for the increased concentration of Cu in the aerated solution when compared to the deaerated one (Table 1).

TABLE 2

The chemical composition of the surface of Al₂Cu electrode after 20.4 h immersion in the 0.5 M H₃PO₄, $T = 295 \text{ K}$

Area in Fig. 3a	Chemical composition, at. %		
	Al	P	Cu
1	23	1	76
2	54	2	44
3	37	2	61
4	42	2	57
5	48	2	50

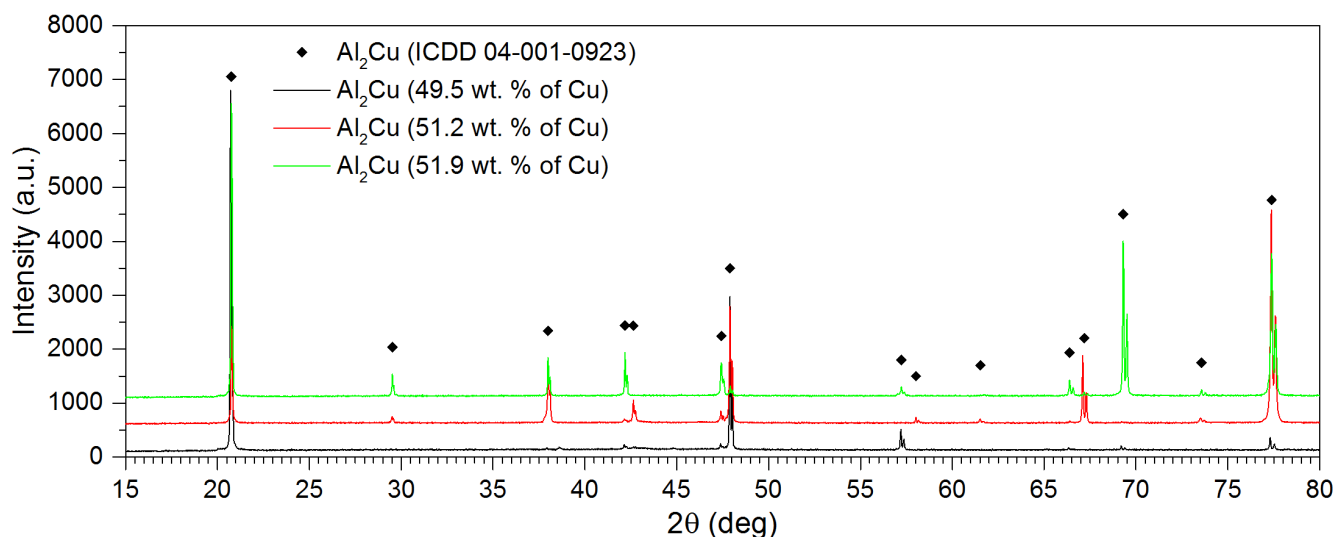


Fig. 2. X-ray diffraction patterns of the alloys obtained, black diamonds indicate the diffraction lines ascribed to the Al₂Cu phase

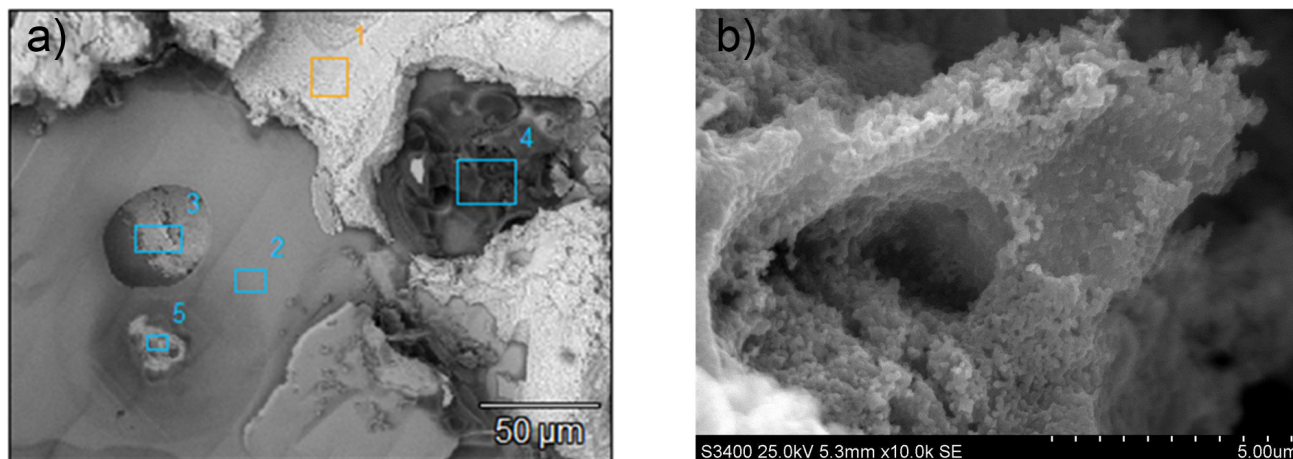


Fig. 3. The surface of Al_2Cu electrode after 20.4 hours of immersion in 0.5 M H_3PO_4 , $T = 295$ K, the areas where the chemical composition was determined are shown, micrograph was obtained by using the backscattered electrons detector (BSE) a), the morphology of the porous, Cu-rich remnant detached from the surface, secondary electrons (SE) detector was used b)

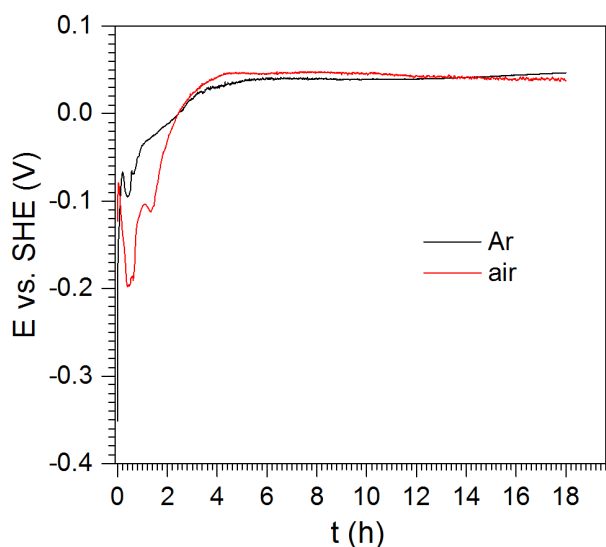


Fig. 4. The corrosion potential of Al_2Cu electrodes immersed in 0.5M H_3PO_4 aqueous solution, $T = 295$ K

Subsequently, the electrochemical methods were applied for better understanding of the corrosion mechanism. Prior polarisation experiments, the open circuit potential vs. immersion time was recorded (Fig. 4). It can be observed that the surface of Al_2Cu phase quickly becomes enriched with copper. It is related with the increase of the electrode potential. The averaged values of corrosion potential (after 20.4 hours) for aerated and deaerated 0.5 M H_3PO_4 solutions are of -14 ± 102 mV vs. SHE and 11 ± 23 mV vs. SHE respectively. The equilibrium potential of the hydrogen electrode is -65 mV vs. SHE ($\text{pH} = 1.1$).

Since the corrosion potential is more positive than the equilibrium potential for hydrogen evolution, the corrosion with hydrogen depolarisation occurs only for a few hours after immersion of the specimens in the solution. Further corrosion is possible due to cathodic reduction of dissolved oxygen or copper ions on the surface of Al_2Cu phase. These processes were investigated by using the linear polarisation method (Fig. 5a). The polarisation curves were recorded in the aerated and deaer-

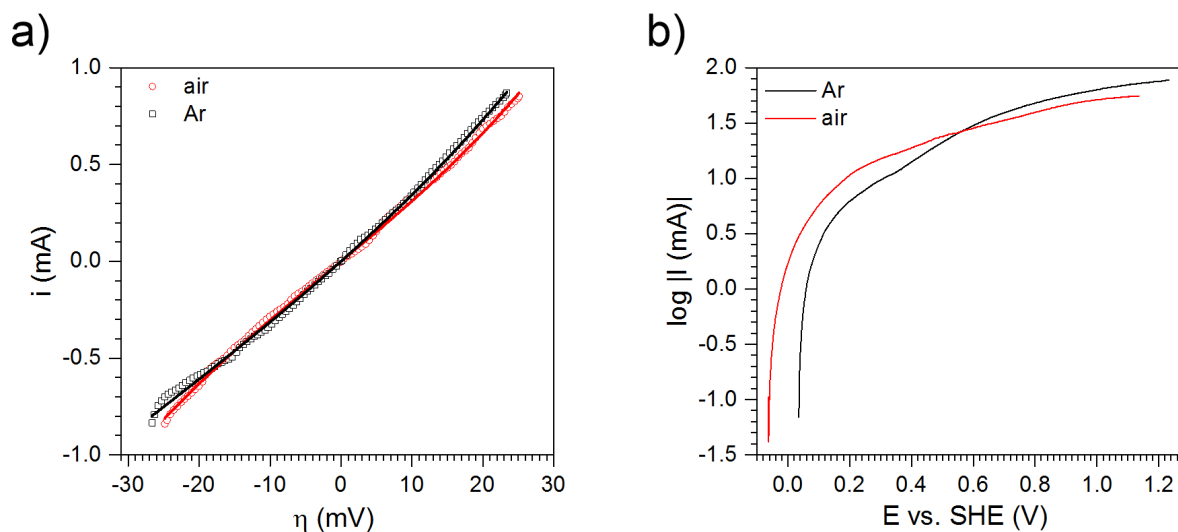


Fig. 5. The polarisation curves of the Al_2Cu electrode in 0.5 M H_3PO_4 , $T = 295$ K as the function of concentration of oxygen in the solution: a) in the vicinity of the corrosion potential, solid lines represent the approximation of the experimental data with the Eq. (2); b) anodic polarisation curves

ated solution, in the vicinity of the corrosion potential. They were subsequently approximated by using the Eq. (2), as it was proposed by Mansfeld [12]:

$$i = \frac{1}{2.303R_p} \frac{\beta_a \beta_c}{\beta_a + \beta_c} \left[\exp\left(\frac{2.303\eta}{\beta_a}\right) - \exp\left(\frac{-2.303\eta}{\beta_c}\right) \right] \quad (2)$$

where R_p is the polarisation resistance, η – overpotential, β_a and β_c – Tafel constants for the anodic and cathodic process respectively. The results obtained are presented in Table 3.

TABLE 3

The results of the approximation of the polarisation curves with the Eq. (2)

Parameter	Value	
	in equilibrium with air	purged with Ar
R_p	$33.1 \pm 0.3 \Omega$	$30.6 \pm 0.3 \Omega$
β_a	$69 \pm 4 \text{ mV}$	$105 \pm 17 \text{ mV}$
β_c	$74 \pm 4 \text{ mV}$	$180 \pm 48 \text{ mV}$
R^2	0.999	0.999

The cathodic process in both cases is reduction of oxygen, dissolved in the electrolyte. The value of Tafel constant ($74 \pm 4 \text{ mV}$) obtained for the solution in equilibrium with air suggests that the limiting step is the charge transfer through the solid/liquid interface. The theoretical value of β_c for this process is equal to 100 mV [12]. However, Cu^{2+} ions are also present in the solution and can be reduced on the surface. Thus, obtained value of β_c accounts for both processes. When the solution was deaerated, the Tafel constant reached much higher value, which indicates that the cathodic process is under diffusion control. The diffusing species are presumably O_2 molecules (due to incomplete deaeration of the solution) and maybe also Cu^{2+} ions, but copper concentration in the solution is very low. It can also be observed that at the sufficient cathodic polarisation (-25 mV), the process of reduction of H_3O^+ originates (cathodic current in Fig. 5a starts to increase).

The anodic polarisation curves, obtained for Al_2Cu phase immersed in $0.5 \text{ M H}_3\text{PO}_4$ aqueous solution, are presented in

Fig. 5b. Their shape suggests active dissolution of the specimens. At the potential above *ca.* 0.4 V vs. SHE , copper is dissolved and subsequently deposited onto the surface of the counter electrodes. In the case of deaerated solution, the current increase around this potential value is clearly visible. It should be noted here that the current density was not calculated, since the real surface area of the electrodes remains unknown. However, it is much bigger when compared to the geometric one (*vide infra*).

Passivity of Al_2Cu phase in acidic solution (0.1 M NaCl , $\text{pH} = 2.5$) has already been reported, however, relatively low value of the corrosion potential (*ca.* -350 mV vs. SHE) was obtained [4]. The discrepancy between the cited results and presented in this work is probably related with the different copper content on the surface due to different aggressiveness of the solutions and probably different immersion time. What is more, when the electrode potential was around 0 V vs. SHE , as it is reported in this work, intermetallic phase underwent corrosion in the transpassive region of the polarisation curve [4]. It supports the observation that Al_2Cu corrodes in the studied solution in the active state.

3.3. EIS characterisation of Al_2Cu phase after the corrosion process

Selective corrosion of the Al_2Cu phase causes its significant porosity. The impedance of the porous electrode was modelled by using the so called “two CPE model”, where CPE stands for constant phase element, composed of two R-CPE loops connected in series. The first, high frequency one is related to the porosity of the electrode, the other one to the charge transfer process [13]. In this work, the capacitor, representing the double layer capacitance C_{dl} was used instead of the low frequency CPE, without deterioration of the fit quality. The approximation of the impedance spectra obtained for different temperature of the solution, by using the “two CPE model” are presented in Fig. 6a. The temperature dependency of R_1 and R_2 is given in Fig. 6b.

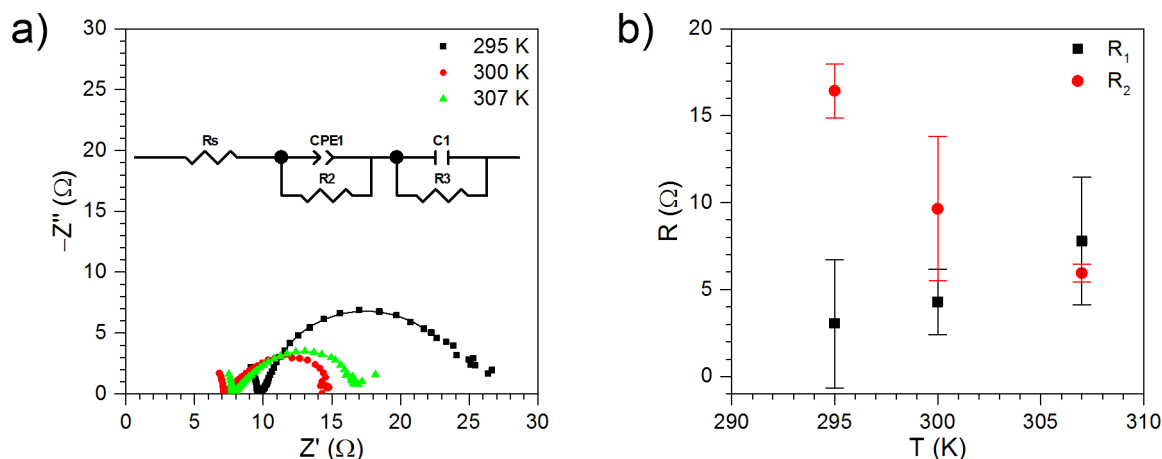


Fig. 6. The impedance spectra of the Al_2Cu electrode in 0.5 M , deaerated, H_3PO_4 as the function of the solution temperature, continuous lines represent their approximation with the equivalent circuit given a), the values of the resistance from the equivalent circuit as the function of the solution temperature b)

It can be concluded that the resistance R_2 decreases with the increasing temperature, contrary to R_1 . Since these results were obtained for deaerated solution, the resistance R_2 was ascribed to the faradaic impedance. It takes into account the charge transfer resistance related with the corrosion process caused by small amount of oxygen and traces of copper in the solution as well as the mass transfer impedance which is related with their diffusion to the surface of the electrode. The double layer capacitance is high due to large surface area of the electrode (high porosity), caused by the selective corrosion process. Moreover, it increases with the increasing temperature due to the higher corrosion rate of the electrode (Fig. 7). The surface area of the electrodes was calculated using the values of C_{dl} obtained, assuming the ideal capacitance of the metallic surface equal to $20 \mu\text{F}\cdot\text{cm}^{-2}$ [13] and neglecting the influence of temperature and pH. The following values were obtained: $2137 \pm 352 \text{ cm}^2$, $3933 \pm 1070 \text{ cm}^2$ and $3896 \pm 1342 \text{ cm}^2$ for 295, 300 and 307 K respectively.

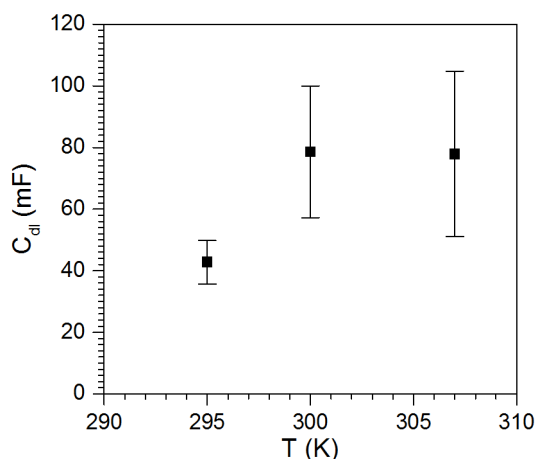


Fig. 7. The capacitance of the double layer as the function of the solution temperature for 0.5 M, deaerated, H_3PO_4

The dependency of the corrosion rate of Al_2Cu phase on the concentration of orthophosphoric acid was also estimated. The impedance spectra obtained for deaerated solutions are

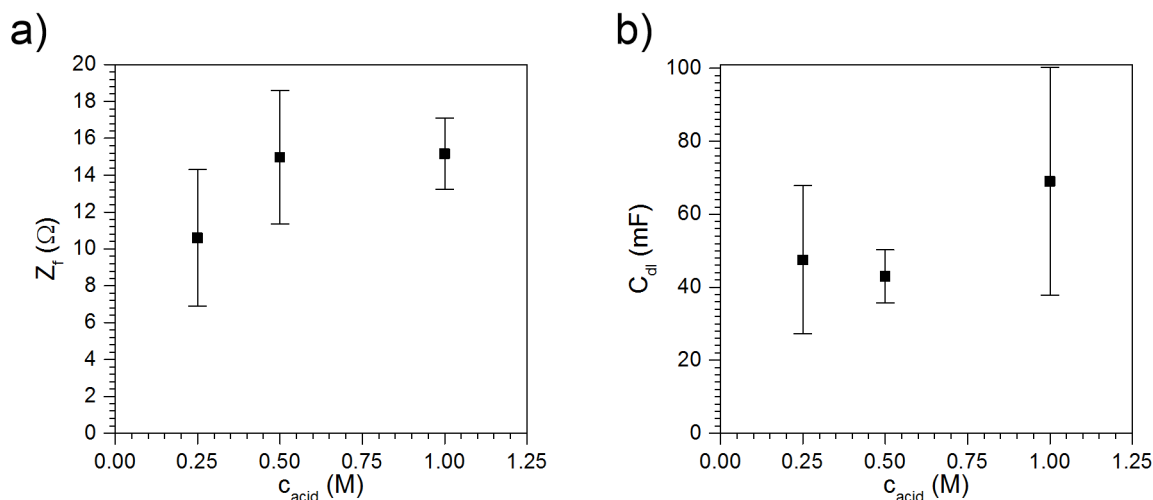


Fig. 9. The values of the faradaic impedance a) and double layer capacitance b) as the function of H_3PO_4 concentration, $T = 295 \text{ K}$, deaerated solution

presented in Fig. 8. They were approximated by using the same equivalent circuit. It is possible to see that the faradaic impedance does not depend on the concentration of H_3PO_4 (Fig. 9a). The capacitance of the double layer also does not change significantly (Fig. 9b). Thus, it can be concluded that the rate of corrosion of Al_2Cu phase virtually does not depend on the concentration of orthophosphoric acid.

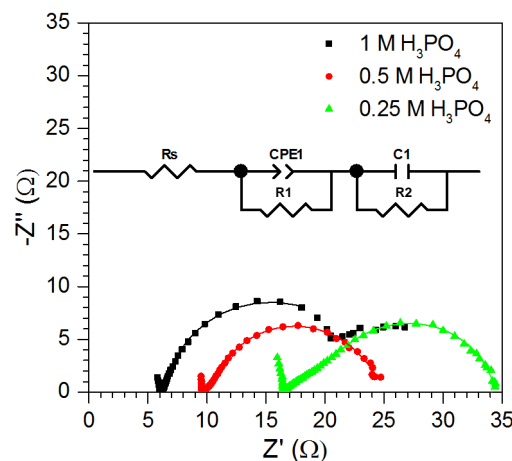


Fig. 8. The impedance spectra of the Al_2Cu electrode as the function of the concentration of orthophosphoric acid, $T = 295 \text{ K}$, continuous lines represent approximation of the spectra

4. Summary

Al_2Cu phase undergoes selective corrosion in 0.5 M H_3PO_4 aqueous solution. The corrosion rate is much higher when compared to aluminium 1050 and 2024 alloy. Oxygen dissolved in the electrolyte behaves as the additional depolariser and increases the corrosion rate of intermetallic phase as well as the concentration of copper in the solution.

The Al_2Cu electrodes after the corrosion process were investigated by using the electrochemical impedance spectroscopy. The impedance spectra were approximated with the so called “two-CPE model”. The faradaic impedance and double

layer capacitance were determined. It was shown that the former decreases whereas the latter increases with the increasing temperature of the solution. The surface area of the Al_2Cu phase after corrosion process was determined as between 2.7 and 4.9 thousand times higher than the geometric value. The increase of the concentration of orthophosphoric acid in the range between 0.25 and 1 M neither increase the surface area of the electrode after corrosion process, nor the faradaic impedance.

Acknowledgment

The financial support from the National Science Centre, Poland, grant no 2016/23/D/ST5/01343 is acknowledged. Authors also acknowledge Mr Kamil Dychtoń and Andrzej Oblój for their help in conducting the electrochemical research and Dr Maciej Pytel for his assistance in analysis of the chemical composition of the solutions.

REFERENCES

- [1] H. Baker, ASM handbook: Alloy phase diagrams, ASM International, Ohio (1992).
- [2] M. Aravind, P. Yu, M.Y. Yau, D.H.L. Ng, Formation of Al_2Cu and AlCu intermetallics in $\text{Al}(\text{Cu})$ alloy matrix composites by reaction sintering, *Mater Sci Eng A*. **380**, 384-393 (2004).
- [3] J.R. Scully, T.O. Knight, R.G. Buchheit, D.E. Peebles, Electrochemical characteristics of the Al_2Cu , Al_3Ta and Al_3Zr intermetallic phases and their relevancy to the localized corrosion of Al alloys, *Corros Sci*. **35**, 185-195 (1993).
- [4] N. Birbilis, R.G. Buchheit, Investigation and discussion of characteristics for intermetallic phases common to aluminum alloys as a function of solution pH, *J Electrochem Soc*. **155**, C117 (2008).
- [5] R.G. Buchheit, A compilation of corrosion potentials reported for intermetallic phases in aluminum alloys, *J Electrochem Soc*. **142**, 3994-3996 (1995).
- [6] W.B. Liu, S.C. Zhang, N. Li, J.W. Zheng, Y.L. Xing, Microporous and Mesoporous Materials A facile one-pot route to fabricate nanoporous copper with controlled hierarchical pore size distributions through chemical dealloying of Al – Cu alloy in an alkaline solution, *Microporous Mesoporous Mater*. **138**, 1-7 (2011).
- [7] S. Lebouil, J. Tardelli, E. Rocca, P. Volovitch, K. Ogle, Dealloying of Al_2Cu , $\text{Al}_7\text{Cu}_2\text{Fe}$, and Al_2CuMg intermetallic phases to form nanoparticulate copper films, *Mater Corros*. **65**, 416-424 (2014).
- [8] L.L. Shreir, R.A. Jarman, G.T. Burstein, *Corrosion*, Butterworth – Heinemann, Oxford (1994).
- [9] P.R. Żabiński, S. Meguro, K. Asami, K. Hashimoto, Electrodeposited Co-Ni-Fe-C Alloys for Hydrogen Evolution in a Hot $8 \text{ kmol}\cdot\text{m}^{-3}$ NaOH, *Mater Trans*. **47**, 2860-2866 (2006).
- [10] P. Kwolek, A. Kamiński, K. Dychtoń, M. Drajewicz, J. Sieniawski, The corrosion rate of aluminium in the orthophosphoric acid solutions in the presence of sodium molybdate, *Corros Sci*. **106**, 208-216 (2016).
- [11] K. Dychtoń, P. Kwolek, The replacement of chromate by molybdate in phosphoric acid-based etch solutions for aluminium alloys, *Corros Eng Sci Technol*. **53**, 234-240 (2018).
- [12] F. Mansfeld, The Polarization Resistance Technique for Measuring Corrosion Currents, in: *Adv Corros Sci Technol*, Plenum Press, (1970).
- [13] L. Chen, A. Lasia, Ni-Al Powder Electrocatalyst for Hydrogen Evolution, *J Electrochem Soc*. **140**, 2464 (1993).